Full length article

Critical media attributes in E-beam sterilization of corneal tissue

Sina Sharifi [a],[*], Hannah Sharifi [a], Ali Akbari [b], Fengyang Lei [a], Claes H. Dohlman [a], Miguel Gonzalez-Andrades [a],[c], Curtis Guild [d], Eleftherios I. Paschalis [a], James Chodosh [a],[*]

[a] *Disruptive Technology Laboratory, Massachusetts Eye and Ear and Schepens Eye Research Institute, Department of Ophthalmology, Harvard Medical School, Boston, MA, USA*
[b] *Solid Tumor Research Center, Research Institute for Cellular and Molecular Medicine, Urmia University of Medical Sciences, Urmia, Iran*
[c] *Maimonides Biomedical Research Institute of Cordoba (IMIBIC), Department of Ophthalmology, Reina Sofia University Hospital and University of Cordoba, Cordoba, Spain*
[d] *Centaur Technologies, Vernon, CT, USA*

ARTICLE INFO

ABSTRACT

When ionizing irradiation interacts with a media, it can form reactive species that can react with the constituents of the system, leading to eradication of bioburden and sterilization of the tissue. Understanding the media's properties such as polarity is important to control and direct those reactive species to perform desired reactions. Using ethanol as a polarity modifier of water, we herein generated a series of media with varying relative polarities for electron beam (E-beam) irradiation of cornea at 25 kGy and studied how the irradiation media's polarity impacts properties of the cornea. After irradiation of corneal tissues, mechanical (tensile strength and modulus, elongation at break, and compression modulus), chemical, optical, structural, degradation, and biological properties of the corneal tissues were evaluated. Our study showed that irradiation in lower relative polarity media improved structural properties of the tissues yet reduced optical transmission; higher relative polarity reduced structural and optical properties of the cornea; and intermediate relative polarity (ethanol concentrations = 20-30% (v/v)) improved the structural properties, without compromising optical characteristics. Regardless of media polarity, irradiation did not negatively impact the biocompatibility of the corneal tissue. Our data shows that the absorbed ethanol can be flushed from the irradiated cornea to levels that are nontoxic to corneal and retinal cells. These findings suggest that the relative polarity of the irradiation media can be tuned to generate sterilized tissues, including corneal grafts, with engineered properties that are required for specific biomedical applications.

Statement of significance

Extending the shelf-life of corneal tissue can improve general accessibility of cornea grafts for transplantation. Irradiation of donor corneas with E-beam is an emerging technology to sterilize the corneal tissues and enable their long-term storage at room temperature. Despite recent applications in clinical medicine, little is known about the effect of irradiation and preservation media's characteristics, such as polarity on the properties of irradiated corneas. Here, we have showed that the polarity of the media can be a valuable tool to change and control the properties of the irradiated tissue for transplantation.

© 2021 Acta Materialia Inc. Published by Elsevier Ltd. All rights reserved.

1. Introduction

Corneal diseases are one of the major causes of vision loss, affecting 4.2% (9.2 million) of the world's blind population (216.6 million) [1] by recent estimates. Corneal allograft surgery (kerato-plasty) is the primary treatment when irreversible cornea structure damage due to disease has occurred. While donor corneas are more available for transplantation in high-resource countries, a severe shortage of high-quality donor tissues persists worldwide, with millions in need of transplantation [2]. Tissue unsuitability, prohibitive cost, allograft rejection and failure, and donor-related infectious complications further compound donor cornea scarcity [3–6]. Significant efforts have been directed to tissue engineering approaches [7–13] including decellularization of xenografts [14,15]

* Corresponding authors.
   E-mail addresses: Sina_Sharifi@meei.harvard.edu (S. Sharifi),
James_Chodosh@meei.harvard.edu (J. Chodosh).

S. Sharifi, H. Sharifi, A. Akbari et al.

to address the global scarcity. Xenografts, though biomechanically and anatomically similar to human tissues, are prone to immune rejection [16–19]. An alternative approach is to generate tissue-engineered scaffolds, but these have not been shown to sufficiently emulate the native cornea's biomechanical properties and molecular architecture to date [10,20]. Presently, the only viable solution to corneal blindness is corneal allograft surgery or use of an artificial cornea (keratoprosthesis, which requires a donor cornea as a carrier to be implanted [21–25].

Extending the shelf-life of explanted corneas, which are normally viable for several weeks if in the appropriate preservation media, could improve the overall accessibility of corneas for transplantation. Sterilizing corneas with ionizing radiation (gamma or electron beam (E-beam)) is an emerging technology that permits long-term tissue storage at room temperature [26–28]. Tissue irradiation leads to the formation of reactive species, which can react to break and/or form new chemical bonds [29]. Such reactions impact the chemical structures of pathogenic contaminants, eradicate bioburden, and sterilize corneal tissue [30,31]. Those reactions also alter the chemical structure of biomacromolecules such as collagen, elastane, etc., present in the tissue, dependent on irradiation type, dosage, and duration [29,32,33]. Irradiation conditions have been suggested to impact the properties of irradiated tissue properties [34,35]. Molecular-level mechanism of how different conditions, including the irradiation media's characteristics, impact native properties of the tissue has not been fully elucidated. One of the most important properties of the media is its polarity [36]. A media with high relative polarity such as water solvates dissolved charged or dipolar species and swells the tissue. The addition of miscible solvents with lower relative polarity (e.g. ethanol) into water reduces the relative polarity of media and induces protein aggregation. This is because the alcohol displaces water from the protein surface and thins the solvation layer around the protein. And with thinner hydration layers, the protein aggregates through attractive electrostatic and dipole forces [37]. To study how relative polarity of the solvent impacts properties of irradiated cornea, we have mixed water (relative polarity of 1.000) with ethanol (relative polarity of 0.654) with varying ratios (100–0% (v/v)) and prepared media with varying relative polarity (1.000–0.654) [38]. After irradiation of corneas in the media with varying relative polarities, we studied their properties after irradiation. Our data show that relative polarity of irradiation media significantly impacts chemical, mechanical, optical, structural, enzymatic degradation, and biological properties of corneal tissue in an ethanol concentration dependent manner.

2. Materials and methods

2.1. Preparation and E-beam irradiation

Fresh porcine eyes were acquired from adult pigs immediately after their death at a local slaughterhouse. After dissecting the porcine corneal tissues (PC), the specimens were immersed in ethanol/water solutions with varying concentrations (0, 10, 20, 30, 40, 50, 60, 70, 80, 90, and 100% (v/v)) and incubated for 24 h to exchange the solvent. After the exchange, the solutions were replaced with fresh solutions of similar composition, then irradiated using a Van de Graaff (Model K) electron accelerator at 2.6 MeV, with a dose rate of 5 kGy per pass and total of 25 kGy (Electron Technology Company; South Windsor, CT). The samples were denoted as PC (non-irradiated control) or E-Beam Irradiated.

2.2. Fourier transform infrared spectroscopy (FT-IR)

For FT-IR measurements, the specimens were first washed with distilled (DI) water, then freeze-dried. FT-IR spectra were col-lected using a Nicolet iS50 FT-IR Spectrometer (Thermo Scientific; Waltham, MA) in the range of 500 to 4000 cm^{-1}, with 64 scans and 0.5 cm^{-1} resolution. A diamond Attenuated Total Reflectance (ATR) accessory on the iS50 was used to collect the spectra.

2.3. Mechanical properties

The mechanical properties of the tissues were determined using a Mark-10 ESM 303 motorized test stand (Mark-10 Corporation, NY, USA) [28]. Prior to testing, specimens were first washed with DI water, then immersed in phosphate-buffered saline (PBS) for 30 min. For the tensile test, corneal tissues were dissected into dumbbell-shaped structures. For testing, initial grip separation was 5 mm, with a crosshead speed of 1 mm/min. Toe and elastic moduli were calculated from the linear derivative of the stress-strain curve in the low stiffness (0–10% strain) and high stiffness range (20–40% strain), respectively. The compression moduli were measured on the same instrument on 6 mm-diameter discs dissected from those groups [$n = 4$]. The moduli were calculated from the linear derivative of the stress-strain curve in the high stiffness range (20–40% strain).

2.4. Optical properties

After washing the tissues with PBS, the optical transmission of trephined corneas (6-mm-diameter central) was assessed in PBS using a UV–Vis. spectrometer (Molecular Devices SpectraMax 384 Plus Microplate Reader, CA, USA). Transmittance spectra (%T) from 300 to 900 nm at 1 nm increments were collected and corrected with PBS blank. For data analysis, values were averaged for $n = 4$, and then quantification was performed by integrating the spectra using OriginLab (Northampton, MA). Contrast was analyzed by optical photography, by which PBS washed specimens were placed on a USAF 1951 (Barrington, NJ) target (group number = -1 and element number = 4). Images were photographed using Dino-Lite camera (AM73915MZTL; Torrance, CA), then analyzed by ImageJ software (NIH, Bethesda, Maryland) from each sample ($n = 4$), and the contrast was calculated according to the following equation:

$$contrast \ (\%) = \frac{[I_{max} - I_{min}]}{[I_{max} + I_{min}]} \ \times \ 100$$

2.5. Relative polarity of media (p_m)

p_m of a binary mixture of ethanol/water can be calculated according to the following equation: $p_m = \phi_1 p_1 + \phi_2 p_2$, where p_m, p_1, and p_2 are the dielectric constants of the binary mixture and solvents 1 and 2, respectively, and ϕ_1 and ϕ_2 are mole fractions of those solvents in the mixture.

2.6. Swelling ratio

Tissue specimens were dissected into 7-mm discs, washed with PBS, blot dried, and weighed (W_i). The specimens were then incubated at 37 °C for 1–24 h immersed in PBS. At defined time points, corneal tissues were blot-dried and re-weighed (W_s). The swelling ratios (S) for the tissues [$n = 4$] were calculated as follows:

$$S \ (\%) = \frac{[W_S - [W_i]}{[W_i]} \times \ 100$$

2.7. In Vitro Biodegradation

Enzymatic degradation of the tissue specimens was assessed using collagenase from Clostridium histolyticum [39]. Briefly, dissected specimens were washed with PBS, then submerged in 0.1 M Tris-HCL buffer (pH = 7.4) containing collagenase (10 U/mL) and

S. Sharifi, H. Sharifi, A. Akbari et al.

CaCl$_2$ (5 mM). The specimens were incubated at 37 °C for 5–20 h, with solution replacement of every 8h. Corneal residues were carefully washed with DI water, lyophilized, and weighed (W_f) to calculate the retaining % [$n = 4$] using the following equation: Retention (%) = $W_f/W_i \times 100$. For the initial weight measurement, the corresponding dissected specimens were washed with PBS, and lyophilized, and weighed (W_i).

2.8. Water contact angle

After PBS washing and blot drying, a drop of DI water (5 µL) was delivered onto the surface of a corneal tissue specimen via a syringe. Then, a high-resolution image was captured from the side using the Dino-Lite Edge camera. The contact angle for each group ($n = 4$) was determined using ImageJ software (NIH, Bethesda, Maryland) [40].

2.9. Glucose diffusion

A Franz cell (9 mm; PermeGear, PA, USA) was employed to assess through-cornea glucose diffusion. After PBS washing and dissecting, specimens were inserted between the two sections of the Franz cell. The top compartment was filled with 1 mL PBS solution, and the bottom was filled with a glucose solution (2000 mg/dL). Both solutions were stirred and held at 37 °C. Diffused glucose concentration in the upper chamber was determined using a Counter Next EZ blood glucometer (Bayer, Parsippany, NJ, USA) to calculate the diffusion coefficients as previously described ($n = 4$) [39].

2.10. Transmission electron microscopy (TEM)

After PBS wash and dissecting the specimens, they were fixed with Karnovsky's fixative (50% strength, pH = 7.4) (Electron Microscopy Sciences, Hatfield, PA) overnight at room temperature. The specimens were first washed with 0.1 M Cacodylate Buffer (Electron Microscopy Sciences) for 5 min, then with PBS (three times). Next, samples were post-fixed with immersion in 2% osmium tetroxide (Electron Microscopy Sciences) for 1.5 h at room temperature. Then they were en bloc stained with 2% aqueous uranyl acetate for 30 min, dehydrated in ethanol, and embedded in epoxy resin (Tousimis, Rockville, MD). 80 nm thin sections were obtained with a Leica EM UC7 ultramicrotome (Leica Microsystems, Buffalo Grove, IL). TEM analysis was obtained at 80 kV using a Hitachi HT7800 TEM, (Tarrytown, NY). Collagen fibril diameter and collagen interfibrillar Brag spacing were quantified using ImageJ software (NIH, Bethesda, MD) from multiple images taken from each sample.

2.11. Live-dead assay

To assess corneal tissue biocompatibility after irradiation the standard Live-Dead assay on human corneal stromal cells (HCS) (kind gift of Dr. J. Jester, UC-Irvine) and human corneal epithelial cells (HCEp) (kind gift of Dr. M. Griffith, University of Montreal), was performed. After PBS washing and dissecting irradiated corneas, specimens were placed in a 48-well tissue culture well plate (TCP). HCS (5000) or HCEp cells (5000) were seeded on each specimen disc suspended in 400 µL of appropriate media [41]. Specimens were incubated at 37 °C and 5% CO$_2$ for up to 7 days, replacing the media every two days. After 1, 4, and 7 days of culture, Live-Dead staining was performed based on the manufacturer's instructions (Life Technologies Carlsbad, CA), followed by fluorescence imaging using an inverted fluorescent microscope (Zeiss Axio Observer Z1; Thornwood, NY). TCP was used as the control group. Cellular viability was determined using ImageJ software ($n = 4$)[42].

2.12. AlamarBlue assay

Metabolic activity of the HCEp and HCS cultured on irradiated corneas was assessed using a standard AlamarBlue assay. After culturing the cells as above, the AlamarBlue assay was performed on days 1, 4, and 7 post culture. At each time point, the media was replaced with 400 µL fresh media containing 0.004% w/v resazurin sodium salt (Sigma-Aldrich, St. Louis, MO), and incubated for 3 h at 37 °C. Then, 200 µL of the media from each well was transferred into a new 96–well plate and read on a BioTek plate reader (Synergy 2, BioTek Instruments) at 560/25 nm for excitation/half-widths and 590/25 nm for emission/half-widths ($n = 4$). TCP was the control group, and fluorescence intensities were corrected for the fluorescence of tissues incubated without cells.

2.13. Statistical analysis

One-way ANOVA with Tukey comparison test in GraphPad Prism Software (GraphPad Software version 8.3.0, CA, USA) was used to compare metabolic activity, collagen fibril diameter, and collagen interfibrillar Brag spacing among the groups. A value of $p \leq 0.05$ was considered statistically significant.

3. Results

3.1. Mechanical properties

Uniaxial stretching of the corneal tissue pre and post treatment showed that the impact of irradiation on the tensile properties of the tissue depends on the ethanol percentage. Irradiation in the absent of ethanol ($E_x = 0$) decreased toe modulus, elastic modulus, and tensile strength from 1.4 ± 0.4 MPa, 11.6 ± 2.6 MPa, and 4.3 ± 0.7 MPa (PC) to 1.4 ± 0.2 MPa, 8.1 ± 1.2 MPa, 3.6 ± 0.5 MPa (E-beam), respectively (Fig. 1a-d). Irradiation in the presence of ethanol increased these properties correlating with ethanol concentration (E_x). The highest toe modulus, elastic modulus, and tensile strength were obtained with irradiation in 100% ethanol ($E_x = 100$) (2.5 ± 0.5 MPa, 28.3 ± 3.8 MPa, and 10.7 ± 1.3 MPa, respectively) as shown in Fig. 1a-d. Irradiation reduced the elongation at break for all tissues; however, the irradiated tissues in high E_x experienced a larger decline (120 ± 10% for PC, 106 ± 12% for $E_x = 0$, and 83 ± 6% for $E_x = 100$) as shown in Fig. 1e. Uniaxial compression showed similar trend to those of tensile with the compression modulus of 2.4 ± 0.3 MPa (PC), 0.7 ± 0.1 MPa ($E_x = 0$), and 4.6 ± 0.4 MPa ($E_x = 100$).
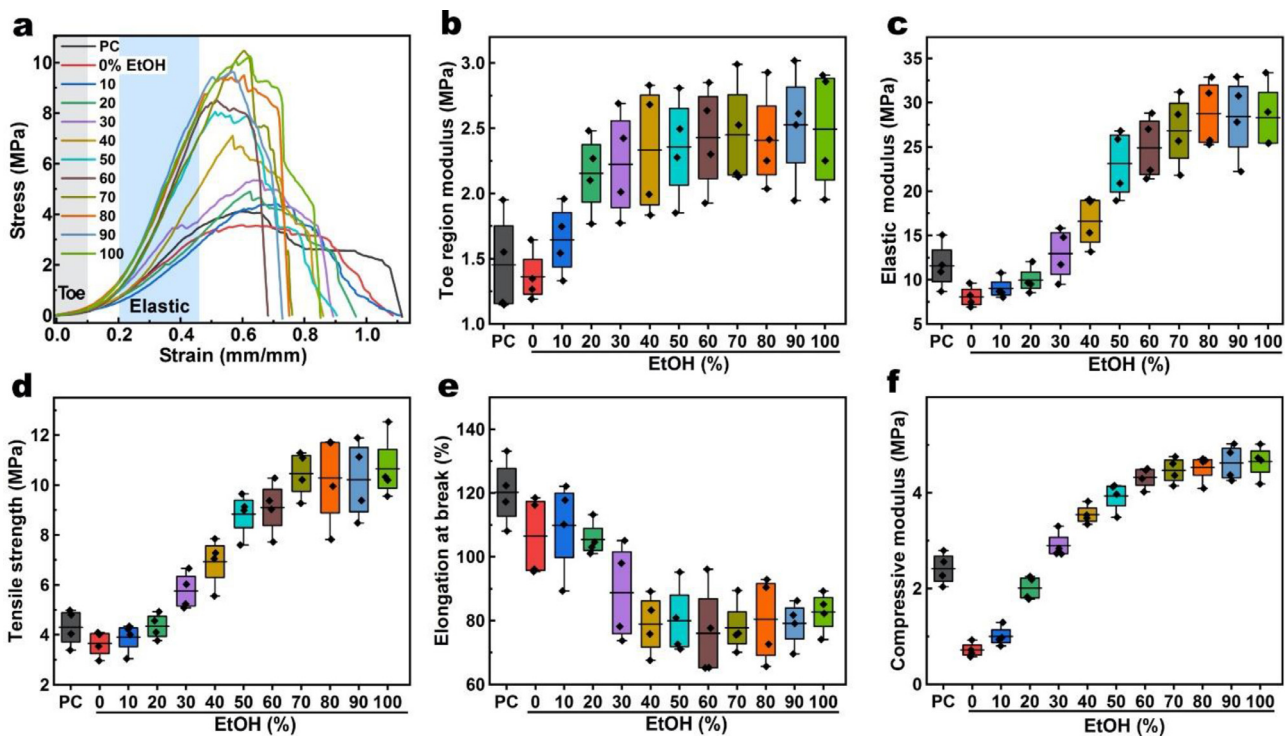
3.2. Optical properties

Absorbance studies showed that irradiation in the absence of ethanol decreased light transmission in both UV and visible ranges from 13 ± 1% and 74 ± 5%, respectively, for PC to 2 ± 0.3% and 50 ± 4% ($E_x = 0$) (Fig. 2a-b). Irradiation in the presence of ethanol ($E_x = 10$) increased the transmittance in both UV and Visible ranges to 14 ± 1% and 83 ± 3%, respectively. Further rise in ethanol content gradually decreased the transmittance in both UV and visible ranges (Fig. 2a-b). There was not any noticeable color change in the corneal tissue upon irradiation in media with any variation of E_{xx} (data not shown). Contrast sensitivity (%) experienced a similar trend as optical transmission: contrast was reduced in the corneal tissue irradiated $E_x = 0$, increased in the lower E_x (e.g. $E_x = 10$), and declined again by further increasing E_x of the media (Fig. 2c-d).

3.3. Chemical and structural characterization

The FT-IR spectra of all groups were almost superimposable (Fig. 3a). However, closer examination showed the amide (I) band

ARTICLE IN PRESS

JID: ACTBIO   [m5G;November 5, 2021;13:28]

S. Sharifi, H. Sharifi, A. Akbari et al.   Acta Biomaterialia xxx (xxxx) xxx

Fig. 1. Characterization of mechanical properties. Representative tensile stress/strain curves of porcine corneas irradiated in the media with varying ethanol concentrations from 0-100% (v/v) (a) and their average toe region moduli (b), elastic (tensile) moduli (c), tensile strength (d), elongation at breaks (e), compared to those of native porcine cornea (PC) along with their corresponding mean compressive moduli (f).
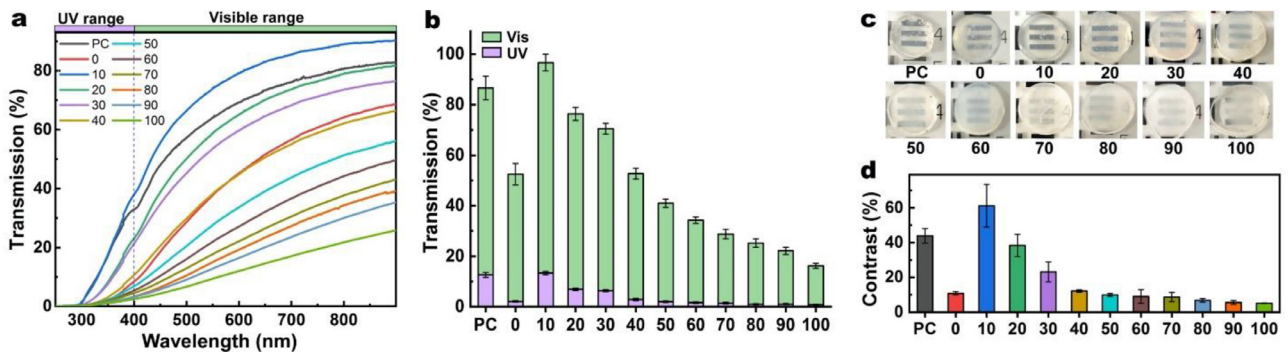
Fig. 2. Optical property analysis. Transmissions irradiated tissues in the media with varying ethanol concentrations from 0-100% (v/v), compared to native PC (a) and their quantifications in both UV (300–400 nm; depicted by violent color) and visible (Vis: 400–900 nm; depicted by green color) range (b). Optical contrast of porcine corneas irradiated in the media with varying ethanol concentrations from 0-100% (v/v), compared to native tissue (c) and their quantifications (d).

slightly blue-shifted from 1639.7 cm^{-1} (PC) to 1644.5 cm^{-1} ($E_x = 0$) (Fig. 3b-c). Irradiation in the presence of ethanol red-shifted the amide (I) band in the E_x dependent manner. The amide vibrational band blue shift suggests that irradiation leads to cleavage of amide bonds to form carboxylic acids and ketones, which have a higher C=O vibrational band in IR (1760–1690 cm^{-1}). The redshift suggests the formation of tyrosine, phenylalanine dimer, indicating the crosslinking of protein chains upon irradiation. The calculation of relative polarity of media shows that increasing E_x, which has lower p (0.654), decreases the overall p_m of the media (Fig. 3d).

3.4. Swelling ratio

Swelling studies showed that irradiated cornea in $E_x = 0$ had similar swelling ratios to those of PC. Irradiated tissues in the presence of ethanol exhibited significantly lower swelling ratios over time in the E_x dependent manner (Fig. 3e). For instance, irradi-

ated corneas in $E_x = 100$ exhibited *ca.* 8% swelling, compared to *ca.* 250% for native PC after 24 h incubation (Fig. 3e).

3.5. Biodegradation

Collagenase-induced biodegradation studies showed the retention of corneal tissue as a function of incubation time (Fig. 3f). While irradiated cornea in $E_x = 0-10$) demonstrated a higher degradation rate than the control (PC), specimens in higher E_x exhibited considerably lower degradation rates (higher stability) compared to control PC. Moreover, control PC was fully digested after 12 h of incubation; however, 10–44% of the residual mass was preserved in the irradiated specimens at $E_x = 20-100$.

3.6. Contract angle measurement

Contact angle studies showed no significant difference between the water contact angle of the cornea before (PC) and after irradiation ($E_x = 0-100$) with p values > 0.6 (Fig. 3g).
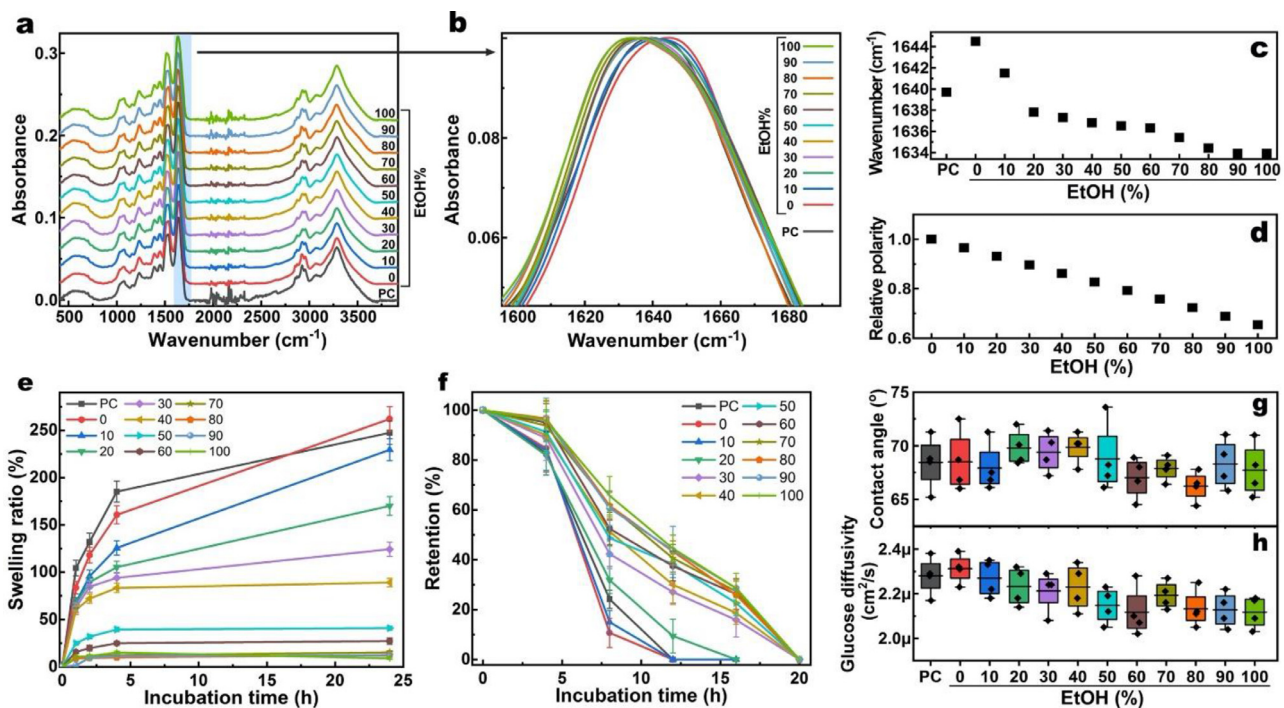
Fig. 3. Chemical and structural analysis. FT-IR spectra of the porcine corneas irradiated in the media with varying ethanol concentration from 0-100% (v/v), compared to PC in full spectral range (450-4000 cm^{-1}) (a) and in the amide (I) vibrational band range (1600-1690 cm^{-1}) (b) and its corresponding vibrational band shift (c). d) Dielectric constants of the media with varying ethanol concentration. Swelling ratio (e), retention in the solution containing collagenous against biodegradation (f) as a function of incubation time, water contact angle (g), and glucose diffusivity (h) for corneas irradiated in the media with varying ethanol/water ratios from 0-100% (v/v), compared to PC.

3.7. Glucose diffusion

Glucose diffusion studies demonstrated that at lower E_x, glucose permeability was similar to those of PC. However, at higher E_x irradiation led to slightly decreased permeability as a function of E_x (Fig. 3h).

3.8. Transmission electron microscopy (TEM)

The structural organization of the anterior, mid, and posterior sections of the corneal stroma, pre, and post-irradiation, are shown in Figure 4a-b. The arrangements of collagen fibrils at both lower and higher magnifications seemed similar among all groups for all three sections. Quantitative high magnification image analysis showed a descending trend in the collagen fibril diameter as a function of ethanol concentration. However, statistical analysis indicated that the collagen fibril diameter of all analyzed sections of the cornea were similar between groups (Fig. 4b-c). Collagen interfibrillar Bragg spacing, on the other hand, seemed to be strongly dependent on the ethanol concentrations of media (Fig. 4b & d) for all three sections. Irradiation in the absence of ethanol increased the collagen interfibrillar Bragg spacing by nearly two-fold. However, irradiation in the present of ethanol retained (lower E_x) or decreased (higher E_x) collagen interfibrillar Bragg spacing.

3.9. Ethanol removal studies

The ethanol removal study showed that the specimens irradiated in higher E_x contained more ethanol, compared to those irradiated in lower E_x (Fig. 5). Our data indicated that the ethanol can be easily removed from the cornea upon immersing in PBS in time dependent manner, with nearly ~96% being removed after rinsing and immersion in PBS for ca. 30 min. This level of residual ethanol is comparable to the ethanol level in cornea after alcohol is normally used in surgery to remove corneal epithelium (Fig. 5).
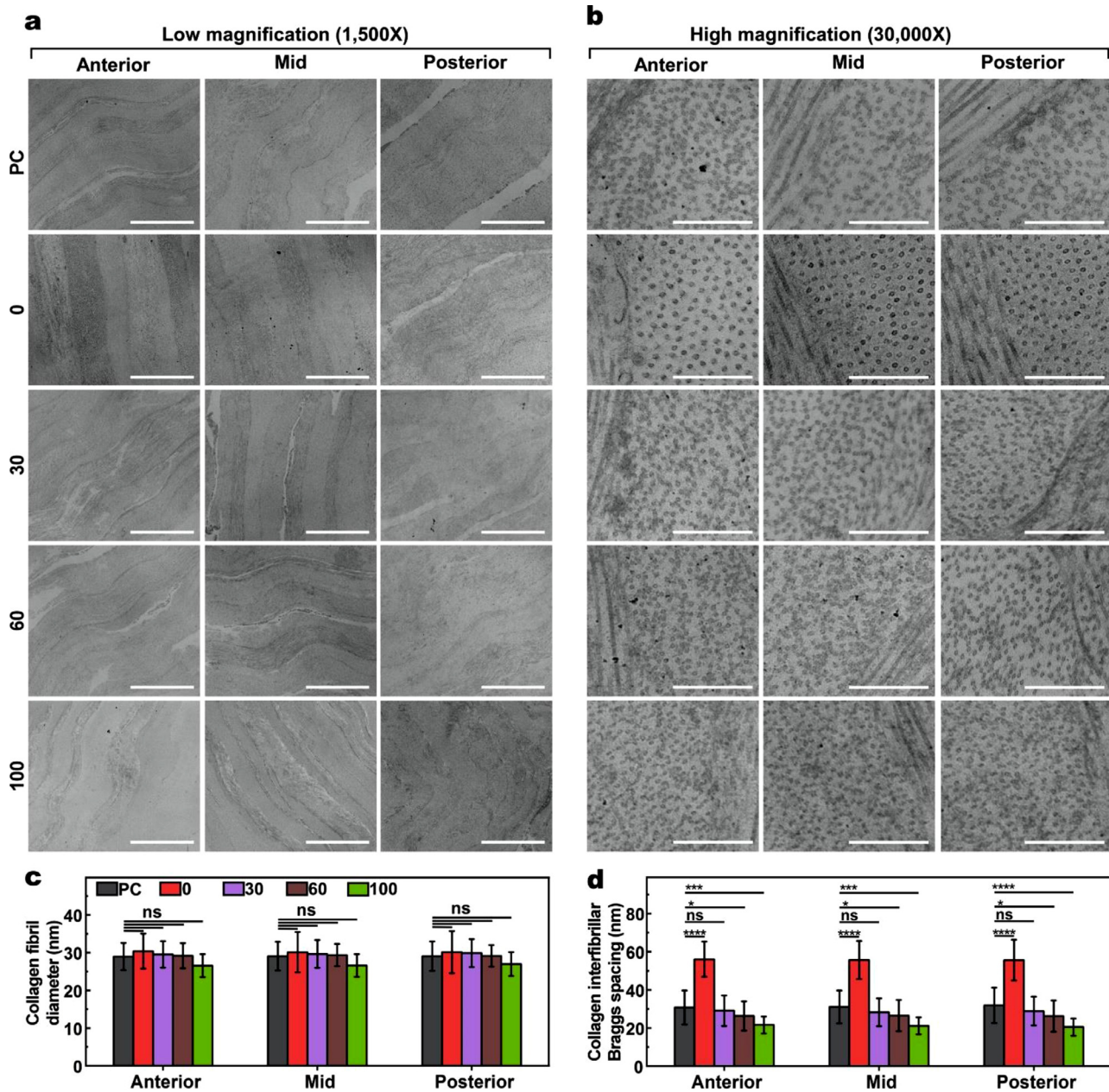
3.10. Residual ethanol cytotoxicity

Cytotoxicity studies indicated that < 5% ethanol present in the media does not cause toxicity to corneal cells, indicated by both Live-Dead and AlamarBlue assays (Fig. S1-S2). These data suggest that if an irradiated cornea (after PBS washing for 30 min) is implanted, any remaining ethanol in the tissue would be inconsequential (Fig. 5), as these values are much lower than the ethanol concentrations that can damage retinal cells (Fig. S3-S4).

3.11. Biocompatibility

Live-Dead assay showed that HCS cultured on irradiated corneas in varying E_x have similar cellular viabilities (>93%) to those cultured on TCP (92 ± 2%) after 7 days of culture. HCS cultured on all samples demonstrated similar cell confluency, spreading pattern, and morphology to those on TCP controls (Fig. 6a-b). HCEp cultured on all irradiated tissues also showed similar viabilities (>91%) to those on TCP (95 ± 5%) after 7 days of culture. HCEp exhibited similar confluency, spreading pattern, and morphology to those of TCP, regardless of E_x of irradiated media (Fig. 6c-d).

AlamarBlue testing of HCS cells seeded on all irradiated cornea in varying E_x demonstrated a gradual increase in relative fluorescence intensity. This indicates relative metabolic activity trend as a function of incubation time, with similar cellular growth and proliferation rate on all experimental samples (Fig. 7a). While HCS seeded on irradiated tissues exhibited slightly lower metabolic activity compared to those on TCP, those differences were not statistically significant ($P > 0.9$). AlamarBlue testing of HCEp cultured on irradiated tissues showed a similar rising trend in relative fluorescence intensity. This increase correlated to incubation time, indicating cellular growth and proliferation occurred in similar fashion on all samples (Fig. 7a). No significant differences in the metabolic activity of cells cultured on irradiated corneas compared to those on TCP were found ($P > 0.95$).

ARTICLE IN PRESS

JID: ACTBIO   [m5G;November 5, 2021;13:28]

S. Sharifi, H. Sharifi, A. Akbari et al.   Acta Biomaterialia xxx (xxxx) xxx
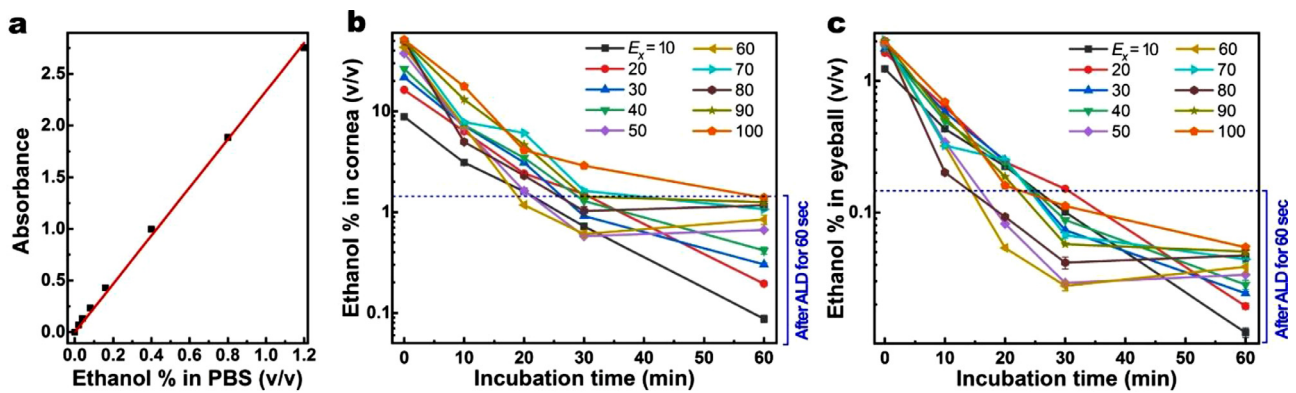
Fig. 4. Transmission electron microscopy (TEM) micrographs of corneal tissues irradiated in the media with varying ethanol concentration (0, 30, 60, and 100% w/w), compared to PC at different layers of the cornea (anterior, mid, and posterior) in low (a) and high (b) magnifications. Quantifications of the collagen fibril diameter (c) and collagen interfibrillar Brag spacing (d). ns, *, **, ***, and **** represent $p \geq 0.05$, $p < 0.05$, $p < 0.01$, $p < 0.001$ and $p < 0.0001$. Scale bars: (a), 10 μm; (b), 0.5 μm.

4. Discussion

Exposing the system to ionizing irradiation such as E-beam can lead to the formation of unstable species (OH˙, H˙, hydroxyethyl radicals, and e_{aq^-}), which can cause irradiation-induced reactions. Some of these may include crosslinking *via* formation of –S–S–, –S–, and –C–C– bonds, if the proteins are sufficiently close (Fig. 8). If the protein chains are not close, the same species may cause hydrolysis of the protein backbone or degradation of amino acid side chains [29,43]. These two competing phenomena (crosslinking and hydrolysis) can impact the chemical, optical, structural, mechanical, and biological properties of irradiated tissues. Our data showed that irradiation of the tissue in E_x = 0–10 negatively affected the mechanical properties of the cornea by reducing its elastic / compressive moduli and tensile strength (Fig. 1). Such weakening of

the tissue indicates that unstable species formed during radiolysis caused amide bond hydrolysis and subsequent chain/fibril scission. However, as E_x increases in the media, the overall relative polarity of media declines, pushing the collagen fibrils closer. This increases the chance of crosslinking upon irradiation and enhances the mechanical properties of the cornea. Our data shows a sigmodal correlation between mechanical behavior and E_x in the media, with the dependence reaching a plateau at the higher ethanol concentrations (E_x = 70) (Fig. 1).

We have previously studied the effect of E-beam irradiation on corneal tissue in recombinant human serum albumin and showed that irradiation had a minimal effect on tissue properties [28]. The effects of E-beam on mechanical properties of bone, bone-tendon-bone, and the anterior cruciate ligament in varying conditions (deep fresh freezing, glycerolisation, and lyophilization, and sub-

ARTICLE IN PRESS

JID: ACTBIO [m5G;November 5, 2021;13:28]

S. Sharifi, H. Sharifi, A. Akbari et al. Acta Biomaterialia xxx (xxxx) xxx

Fig. 5. Ethanol concentration assessment. a) calibration plot to find the concentration of ethanol in PBS solution. Remaining ethanol content in the irradiate cornea (b) and calculated ethanol concentrations in the eyeball after implantation (c) as a function of incubation time, compared to assessed ethanol content of the cornea and eyeball after alcohol-assisted delamination (ALD) of the corneal epithelium with 20% alcohol after 60 seconds of exposure. After 30 min of soaking, the ethanol content of the irradiated cornea drops to a level that is less than that of cornea when ALD is normally used to remove corneal epithelium.
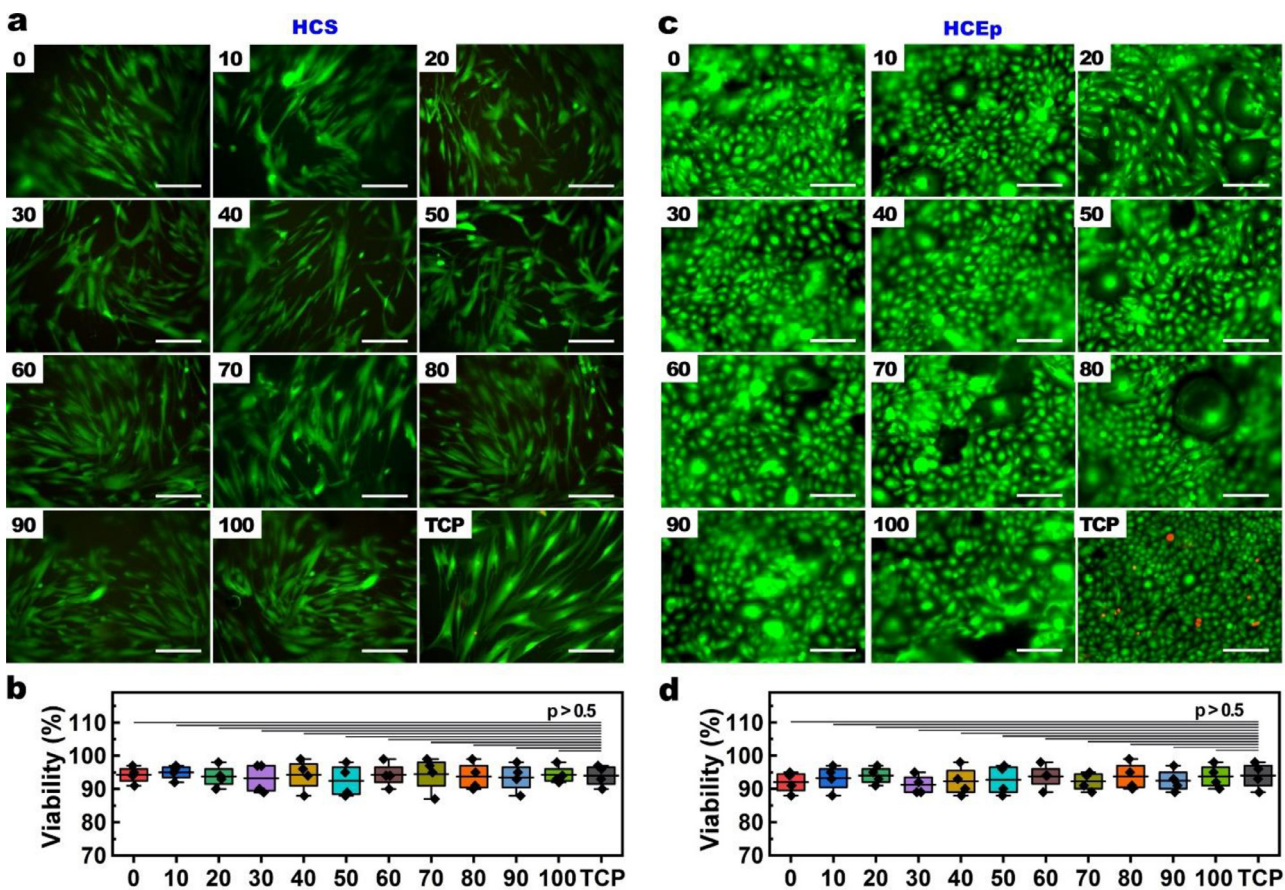
Fig. 6. Biocompatibility of hybrid constructs. Representative Live-Dead images (a) and viabilities (b) of HCS cells cultured on porcine corneas irradiated in the media with varying ethanol/water ratios from 0-100% (v/v) compared to tissue culture well plate (TCP). Representative Live-Dead images (c) and viability (d) of HCEp cultured on porcine corneas irradiated in the media with varying ethanol/water ratios from 0-100% (v/v) compared to tissue culture well plate (TCP). Green (calcein-AM): live cells and red (ethidium homodimer-1): dead cells. Scale bar: 200 μm.

sequent irradiation) have been previously studied [34,35]. Irradiation conditions were shown to significantly impact biomechanical properties of the irradiated tissues, with some authors suggesting that irradiation has the least impact on biomechanical properties of deep-frozen grafts [34,35]. Moreover, while irradiation dropped the tensile strength of frozen radiation-sterilized grafts by ~20%, the authors did not note any significant dose-related differences in the investigated dose range of 25–100 kGy [34]. However, others noted that high-dose E-beam irradiation damaged the biome-

chanics of the soft tissue allograft [44]. This discrepancy can be attributed to the fact that those tissues in different reports might have undergone irradiation at a different stage of swelling in which collagen/elastin fibers have varying distances. Such varying distances can tip the balance between protein crosslinking and hydrolysis and consequently impact the structural properties of the irradiated tissues.

Optical transmission and contrast studies show that irradiation of the cornea in the absence of ethanol changes its optical proper-
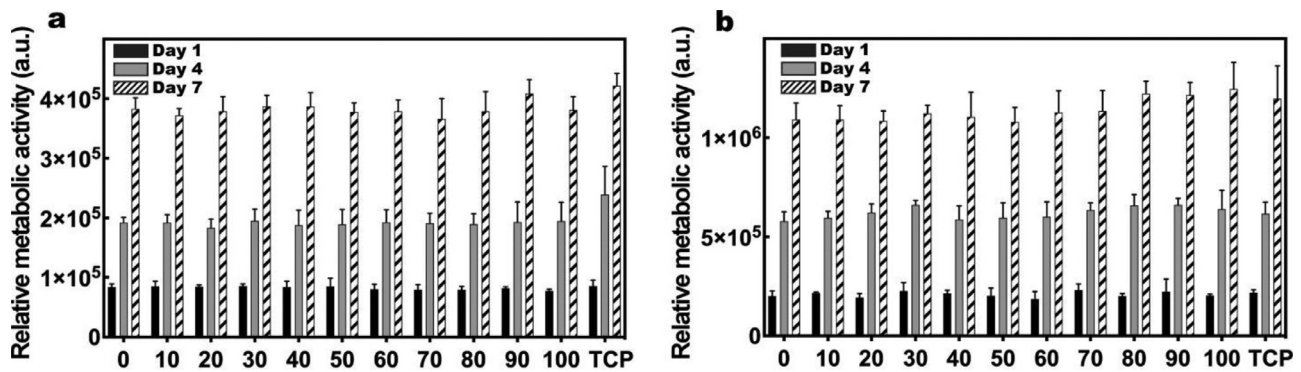
Fig. 7. Quantification of the metabolic activity of (a) HCS and (b) HCEp cultured on PC irradiated in the media with varying ethanol concentrations from 0-100% (v/v) compared to those on tissue culture well plate (TCP) after 1, 4, and 7 days of cell culture, using AlamarBlue assay.
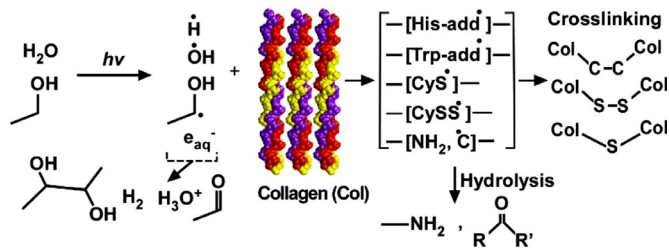

Fig. 8. Schematic of chemical species generated in the radiolysis of ethanol/water solution and their reaction with proteins (collagen) present in the solution.

ties (Fig. 2), because of swelling as previously suggested [27]. The addition of ethanol with a low percentage ($E_x = 10$-20) prevents tissue swelling and retains or even improves the optical properties upon irradiation. However, higher E_x ($E_x = 30$–100) can cause protein aggregation, leading to light scattering and consequently to reduced light transmission and contrast [45]. Transparency of the transplant is crucial if the irradiated transplant is used in either partial-thickness (lamellar,) or full-thickness (penetrating) keratoplasty [46–48]. For such cases, the corneal grafts should be irradiated in media with a low percentage of ethanol ($E_x = 10$–20). However, to irradiate a cornea for use as a carrier for a keratoprosthesis does not require optical transparency but rather structural integrity to avoid keratolysis [24,25,49–53], which can lead to aqueous leakage, hypotony, infection, suprachoroidal hemorrhage, and prosthesis extrusion [21–23]. Irradiation of corneal graft in media with a high percentage of ethanol ($E_x > 30$) can be beneficial, as irradiation can crosslink the cornea, as also shown by FT-IR analysis (Fig 3a-c). This may inhibit keratolysis as previously indicated [54].

The swelling ratios of the irradiated corneas in varying E_x were lower in an E_x dependent manner (Fig. 3e). This observation complements the structural, optical, and chemical analyses, suggesting E-beam induces crosslinking of collagen fibrils in the presence of ethanol [55]. Such crosslinking likely accounts for higher stability of the irradiated corneas against enzymatic biodegradation compared to controls (Fig. 3f) [55, 56]. During adaptive matrix remodeling, stromal cells secrete factors that either promote synthesis or degradation of the extracellular matrix. Overly rapid degradation can lead to premature loss of graft properties before new tissue has formed, resulting in implant failure [57]. Our study to assess the glucose permeability of corneas before and after irradiation showed that the irradiation impact on the glucose diffusion is insignificant, though increasing E_x in the media seems to slightly reduce the permeability. On this basis, we suggest irradiation should not contribute to keratolysis (Fig. 3h).

Ultrastructural analysis suggested that irradiation of cornea tissues at varying E_x does not have a statistically significant on collagen fibril diameter. (Fig. 4b-c). However, irradiation did affect the collagen interfibrillar Bragg spacing in an E_x dependent manner (Fig. 4b & d). Such dependency is believed to stem from the swelling properties of the cornea in varying E_x. In the absent of ethanol, the tissue swells, leading collagen fibrils to dilate. In the presence of ethanol, the tissue shrinks, leading collagen fibrils to contract. The irradiation of those dilated or contracted collagen fibrils leads to hydrolysis or crosslinking and subsequent softening or solidification of those fibrils as also suggested by chemical and mechanical studies. These data complement the structural and mechanical analysis and indicate an intimate relationship between the polarity of the irradiation media and structural properties of the tissue.

Host corneal stromal cells need to favorably interact with the donor implant to be able to migrate into the implant, adhere, proliferate, and produce extracellular matrix, regenerating healthy corneal tissue in its place [10,39]. Host corneal epithelial cells should also be able to migrate onto and adhere to the transplant to proliferate and form a healthy, stratified corneal epithelium. A failure in any of these processes may result in loss of implant [58]. A failure to recover epithelium or damage to the epithelial layer can lead to production of proteases, cytokines, and growth factors from the lacrimal gland, corneal cells, and circulating inflammatory cells. A balanced ratio of these proteins leads to healing, while unbalanced synthesis of those proteins can interfere with epithelial healing and enhance protease action, causing gradual destruction of the corneal structure and ultimately ulceration [59]. Our *in vitro* data showed the irradiation of cornea in ethanol did not impact the viability, proliferation, or metabolic activity of human corneal cells (HCS and HCEp) (Figs. 6-7). This data indicates that the corneal tissues retained their biological properties upon irradiation. Though irradiation may generate some toxic compounds such as H_2O_2, those compounds either have low concentrations, which would have a minimal impact on the biological activity of the implant, or during the washing process were eliminated because of their smaller size, rapid diffusion, and high solubility in water. The absorbed ethanol in the irradiated cornea could be easily and quickly eluted out in PBS solution at room temperature prior to implantation. Therefore, a simple washing step can prevent any possible ocular toxicity of ethanol [60–63].

The preservation of E-beam irradiated corneas in recombinant human serum albumin is FDA-approved, and E-beam irradiated corneas are currently marketed and in use for many routine surgeries, including glaucoma shunt covers and lamellar corneal patch grafts [26,27]. Long-term survival of an E-beam irradiated corneal implant relies not only on the characteristics of the irradiated tissue itself, but also local and systemic factors as governed by the ocular surface milieu and preexisting disease condition. Chemical analysis of corneas that were E-beam irradiated in ethanol did not show any covalent incorporation of ethanol within the corneal

grafts, and therefore, we do not expect that addition of ethanol to the irradiation media will have a negative impact on the biocompatibility of grafts or their survival over time. Rather, the particular biochemical composition, inflammatory state, and microarchitecture of the surrounding extracellular matrix and arrangement of cells in the tissue, their relationships, and their physiological interactions all dictate cell behavior under *in vivo* conditions that cannot be fully simulated *in vitro*. To understand whether the presence of ethanol in the irradiation media impacts biocompatibility of the corneal implant *in vivo*, the critical next step is to study the interactions of the irradiated corneal graft with host tissue in an animal model.

5. Conclusion

The impact of E-beam irradiation in the structural, chemical, mechanical, and optical properties of the cornea depend on the ethanol concentration in water or relative polarity of the media. We found that the irradiation in the media with low relative polarity enhances structural and mechanical properties of the cornea yet reduces its optical transparency and contrast. Irradiation in the media with high relative polarity (*e.g.* water) downgrades structural, mechanical, and optical properties of the cornea. Irradiation in media with an intermediate range of polarity ($E_x = 20$–30) slightly improves the structural and mechanical properties yet retains the optical properties of the cornea compared to native tissue. Regardless, irradiation does not seem to impact the biocompatibility of the corneal graft. Varying the polarity of the irradiation media may enable the tuning of structural, mechanical, chemical, and optical properties of not only corneal grafts but potentially other tissues; many of which currently suffer from the decline of native properties after irradiation [44]. Optimizing E-beam irradiation condition not only achieves sterilization of tissue and its preservation for an extended time at room temperature and consequently can help to address challenges associated with the lack of donor corneas globally, but also enables modulation of properties of the tissue based on specific medical needs.

Declaration of Competing Interest

The authors declare no conflict of interest.

Supplementary materials

Supplementary material associated with this article can be found, in the online version, at doi:10.1016/j.actbio.2021.10.033.

References

[1] S.R. Flaxman, R.R.A. Bourne, S. Resnikoff, P. Ackland, T. Braithwaite, M.V. Cicinelli, A. Das, J.B. Jonas, J. Keeffe, J.H. Kempen, J. Leasher, H. Limburg, K. Naidoo, K. Pesudovs, A. Silvester, G.A. Stevens, N. Tahhan, T.Y. Wong, H.R. Taylor, R. Bourne, P. Ackland, A. Arditi, Y. Barkana, B. Bozkurt, T. Braithwaite, A. Bron, D. Budenz, F. Cai, R. Casson, U. Chakravarthy, J. Choi, M.V. Cicinelli, N. Congdon, R. Dana, R. Dandona, L. Dandona, A. Das, I. Dekaris, M. Del Monte, J. deva, L. Dreer, L. Ellwein, M. Frazier, K. Frick, D. Friedman, J. Furtado, H. Gao, G. Gazzard, R. George, S. Gichuhi, V. Gonzalez, B. Hammond, M.E. Hartnett, M. He, J. Hejtmancik, F. Hirai, J. Huang, A. Ingram, J. Javitt, J. Jonas, C. Joslin, J. Keeffe, J. Kempen, M. Khairallah, R. Khanna, J. Kim, G. Lambrou, V.C. Lansingh, P. Lanzetta, J. Leasher, J. Lim, H. Limburg, K. Mansouri, A. Mathew, A. Morse, B. Munoz, D. Musch, K. Naidoo, V. Nangia, M. Palaiou, M.B. Parodi, F.Y. Pena, K. Pesudovs, T. Peto, H. Quigley, M. Raju, P. Ramulu, Z. Rankin, S. Resnikoff, D. Reza, A. Robin, L. Rossetti, J. Saaddine, M. Sandar, J. Serle, T. Shen, R. Shetty, P. Sieving, J.C. Silva, A. Silvester, R.S. Sitorus, D. Stambolian, G. Stevens, H. Taylor, J. Tejedor, J. Tielsch, M. Tsilimbaris, J. van Meurs, R. Varma, G. Virgili, Y.X. Wang, N.-L. Wang, S. West, P. Wiedemann, T. Wong, R. Wormald, Y. Zheng, Global causes of blindness and distance vision impairment 1990–2020: a systematic review and meta-analysis, Lancet Global Health 5 (12) (2017) e1221–e1234.

[2] P. Gain, R. Jullienne, Z. He, M. Aldossary, S. Acquart, F. Cognasse, G. Thuret, Global survey of corneal transplantation and eye banking, JAMA Ophthalmol. 134 (2) (2016) 167–173.

[3] H. Hara, D.K. Cooper, Xenotransplantation–the future of corneal transplantation? Cornea 30 (4) (2011) 371–378.

[4] Y. Qazi, P. Hamrah, Corneal allograft rejection: immunopathogenesis to therapeutics, J. Clin. Cell Immunol. 2013 (Suppl 9) (2013).

[5] W. Stevenson, S.-F. Cheng, P. Emami-Naeini, J. Hua, E.I. Paschalis, R. Dana, D.R. Saban, Gamma-irradiation reduces the allogenicity of donor corneas, Investigat. Ophthalmol. Visual Sci. 53 (11) (2012) 7151–7158.

[6] M.M. Islam, R. Sharifi, M. Gonzalez-Andrades, Corneal tissue engineering, in: J.L. Alió, J.L. Alió del Barrio, F. Arnalich-Montiel (Eds.), Corneal Regeneration: Therapy and Surgery, Springer International Publishing, Cham, 2019, pp. 23–37.

[7] M. Griffith, B.K. Poudel, K. Malhotra, N. Akla, M. González-Andrades, D. Courtman, V. Hu, E.I. Alarcon, Biosynthetic alternatives for corneal transplant surgery, Expert Rev. Ophthalmol. 15 (3) (2020) 129–143.

[8] P. Rama, S. Matuska, G. Paganoni, A. Spinelli, M. De Luca, G. Pellegrini, Limbal stem-cell therapy and long-term corneal regeneration, N. Engl. J. Med. 363 (2) (2010) 147–155.

[9] I. Brunette, C.J. Roberts, F. Vidal, M. Harissi-Dagher, J. Lachaine, H. Sheardown, G.M. Durr, S. Proulx, M. Griffith, Alternatives to eye bank native tissue for corneal stromal replacement, Prog. Retin Eye Res. 59 (2017) 97–130.

[10] P. Fagerholm, N.S. Lagali, K. Merrett, W.B. Jackson, R. Munger, Y. Liu, J.W. Polarek, M. Soderqvist, M. Griffith, A biosynthetic alternative to human donor tissue for inducing corneal regeneration: 24-month follow-up of a phase 1 clinical study, Sci. Transl. Med. 2 (46) (2010) 46ra61.

[11] F. Li, D. Carlsson, C. Lohmann, E. Suuronen, S. Vascotto, K. Kobuch, H. Sheardown, R. Munger, M. Nakamura, M. Griffith, Cellular and nerve regeneration within a biosynthetic extracellular matrix for corneal transplantation, P Natl. Acad. Sci. USA 100 (26) (2003) 15346–15351.

[12] L.E.R. O'Leary, J.A. Fallas, E.L. Bakota, M.K. Kang, J.D. Hartgerink, Multi-hierarchical self-assembly of a collagen mimetic peptide from triple helix to nanofibre and hydrogel, Nat. Chem. 3 (10) (2011) 821–828.

[13] G. Yazdanpanah, R. Shah, S. Raghurama, R Somala, K.N. Anwar, X. Shen, S. An, M. Omidi, M.I. Rosenblatt, T. Shokuhfar, A.R. Djalilian, In-situ porcine corneal matrix hydrogel as ocular surface bandage, Ocular Surf. 21 (2021) 27–36.

[14] M.M. Islam, R. Sharifi, S. Mamodaly, R. Islam, D. Nahra, D.B. Abusamra, P.C. Hui, Y. Adibnia, M. Goulamaly, E.I. Paschalis, A. Cruzat, J Kong, P.H. Nilsson, P. Argueso, T.E. Mollnes, J. Chodosh, C.H. Dohlman, M. Gonzalez-Andrades, Effects of gamma radiation sterilization on the structural and biological properties of decellularized corneal xenografts, Acta Biomater. 96 (2019) 330–344.

[15] R. Sharifi, Y. Yang, Y. Adibnia, C.H. Dohlman, J. Chodosh, M. Gonzalez-Andrades, Finding an optimal corneal xenograft using comparative analysis of corneal matrix proteins across species, Sci. Rep.-Uk 9 (1) (2019) 1876.

[16] S.F. Badylak, Decellularized allogeneic and xenogeneic tissue as a bioscaffold for regenerative medicine: factors that influence the host response, Ann. Biomed. Eng. 42 (7) (2014) 1517–1527.

[17] D.D. Cissell, J.C. Hu, L.G. Griffiths, K.A. Athanasiou, Antigen removal for the production of biomechanically functional, xenogeneic tissue grafts, J. Biomech. 47 (9) (2014) 1987–1996.

[18] J.H. Lawson, J.L. Platt, Molecular barriers to xenotransplantation, Transplantation 62 (3) (1996) 303–310.

[19] T.W. Gilbert, T.L. Sellaro, S.F. Badylak, Decellularization of tissues and organs, Biomaterials 27 (19) (2006) 3675–3683.

[20] M.M. Islam, O. Buznyk, J.C. Reddy, N. Pasyechnikova, E.I. Alarcon, S. Hayes, P. Lewis, P. Fagerholm, C.L. He, S. Iakymenko, W.G. Liu, K.M. Meek, V.S. Sangwan, M. Griffith, Biomaterials-enabled cornea regeneration in patients at high risk for rejection of donor tissue transplantation, NPJ Regen. Med. 3 (2018).

[21] J. Park, P. Phrueksaudomchai, M.S. Cortina, Retroprosthetic membrane: a complication of keratoprosthesis with broad consequences, Ocul. Surf. 18 (4) (2020) 893–900.

[22] R. Daoud, S. Sabeti, M. Harissi-Dagher, Management of corneal melt in patients with Boston Keratoprosthesis Type 1: Repair versus repeat, Ocul. Surf. 18 (4) (2020) 713–717.

[23] L.N. Kanu, M. Niparugs, M. Nonpassopon, F.I. Karas, J.M. de la Cruz, M.S. Cortina, Predictive factors of Boston type I keratoprosthesis outcomes: a long-term analysis, Ocul. Surf. 18 (4) (2020) 613–619.

[24] M.S. Cortina, F.I. Karas, C. Bouchard, A.A. Aref, A. Djalilian, T.S. Vajaranant, Staged ocular fornix reconstruction for glaucoma drainage device under neoconjunctiva at the time of Boston type 1 Keratoprosthesis implantation, Ocul. Surf. 17 (2) (2019) 336–340.

[25] S. Jabbehdari, T.W. Starnes, K.H. Kurji, M. Eslani, M.S. Cortina, E.J. Holland, A.R. Djalilian, Management of advanced ocular surface disease in patients with severe atopic keratoconjunctivitis, Ocul. Surf. 17 (2) (2019) 303–309.

[26] R. Singh, D. Singh, A. Singh, Radiation sterilization of tissue allografts: a review, World J. Radiol. 8 (4) (2016) 355–369.

[27] K.D. Tran, Y. Li, J.D. Holiman, M. Tang, D. Huang, M.D. Straiko, C.G. Stoeger, Light scattering measurements in electron-beam sterilized corneas stored in recombinant human serum albumin, Cell Tissue Bank 19 (1) (2018) 19–25.

[28] S. Sharifi, H. Sharifi, C. Guild, M.M. Islam, K.D. Tran, C. Patzer, C.H. Dohlman, E.I. Paschalis, M. Gonzalez-Andrades, J. Chodosh, Toward electron-beam sterilization of a pre-assembled Boston keratoprosthesis, Ocul. Surf. 20 (2021) 176–184.

[29] W.M. Garrison, Reaction mechanisms in the radiolysis of peptides, polypeptides, and proteins, Chem. Rev. 87 (2) (1987) 381–398.

[30] M. Silindir Gunay, Y. Ozer, Sterilization methods and the comparison of E-Beam sterilization with gamma radiation sterilization, FABAD J. Pharm. Sci. 34 (2009) 43–53.

[31] A. Hoburg, S. Keshlaf, T. Schmidt, M. Smith, U. Gohs, C. Perka, A. Pruss, S. Scheffler, Effect of electron beam irradiation on biomechanical properties of patellar tendon allografts in anterior cruciate ligament reconstruction, Am. J. Sports Med. 38 (2010) 1134–1140.

[32] J.G. Drobny, 2 - Fundamentals of radiation chemistry and physics, in: J.G. Drobny (Ed.), Ionizing Radiation and Polymers, William Andrew Publishing 2013, pp. 11-26.

[33] M. Silindir Gunay, Y. Ozer, Sterilization methods and the comparison of E-Beam sterilization with gamma radiation sterilization, Fabad J. Pharm. Sci. 34 (2009) 43–53.

[34] A. Kaminski, G. Gut, J. Marowska, M. Lada-Kozlowska, W. Biwejnis, M. Zasacka, Mechanical properties of radiation-sterilised human bone-tendon-bone grafts preserved by different methods, Cell Tissue Bank 10 (3) (2009) 215–219.

[35] G. Gut, J. Marowska, A. Jastrzebska, E. Olender, A. Kaminski, Structural mechanical properties of radiation-sterilized human bone-tendon-bone grafts preserved by different methods, Cell Tissue Bank 17 (2) (2016) 277–287.

[36] A.R. Katritzky, D.C. Fara, H. Yang, K. Tämm, T. Tamm, M. Karelson, Quantitative Measures of Solvent Polarity, Chem. Rev. 104 (1) (2004) 175–198.

[37] E.J. Cohn, L.E. Strong, W.L. Hughes, D.J. Mulford, J.N. Ashworth, M. Melin, H.L. Taylor, Preparation and properties of serum and plasma proteins. IV. A system for the separation into fractions of the protein and lipoprotein components of biological tissues and fluids, J. Am. Chem. Soc. 68 (3) (1946) 459–475.

[38] C. Reichardt, Empirical Parameters of Solvent Polarity, Solvents and Solvent Effects in Organic Chemistry, Wiley-VCH Publishers 2002, pp. 389-469.

[39] S. Sharifi, M.M. Islam, H. Sharifi, R. Islam, D. Koza, F. Reyes-Ortega, D. Alba–Molina, P.H. Nilsson, C.H. Dohlman, T.E. Mollnes, J. Chodosh, M. Gonzalez-Andrades, Tuning gelatin-based hydrogel towards bioadhesive ocular tissue engineering applications, Bioact. Mater. 6 (11) (2021) 3947–3961.

[40] R. Sharifi, S. Mahmoudzadeh, M.M. Islam, D. Koza, C.H. Dohlman, J. Chodosh, M. Gonzalez-Andrades, Covalent functionalization of pmma surface with l-3,4-dihydroxyphenylalanine (L-DOPA) to enhance its biocompatibility and adhesion to corneal tissue, Adv. Mater. Interfaces 7 (2020) 1900767.

[41] S. Sharifi, M.M. Islam, H. Sharifi, R. Islam, T.N. Huq, P.H. Nilsson, T.E. Mollnes, K.D. Tran, C. Patzer, C.H. Dohlman, H.K. Patra, E.I. Paschalis, M. Gonzalez-Andrades, J. Chodosh, Electron beam sterilization of poly(methyl methacrylate)-physicochemical and biological aspects, Macromol. Biosci. 21 (4) (2021) e2000379.

[42] S. Sharifi, M.M. Islam, H. Sharifi, R. Islam, P.H. Nilsson, C.H. Dohlman, T.E. Mollnes, E.I. Paschalis, J. Chodosh, Sputter deposition of titanium on poly(methyl methacrylate) enhances corneal biocompatibility, Transl. Vis. Sci. Technol. 9 (13) (2020) 41.

[43] E. Achilli, M. Siri, C.Y. Flores, P.A. Kikot, S. Flor, M. Martinefski, S. Lucangioli, S.d.V. Alonso, M. Grasselli, Radiolysis effect of the high proportion of ethanol in the preparation of albumin nanoparticle, Radiat. Phys. Chem. 165 (2019) 108387.

[44] T. Schmidt, A. Hoburg, C. Broziat, M.D. Smith, U. Gohs, A. Pruss, S. Scheffler, Sterilization with electron beam irradiation influences the biomechanical properties and the early remodeling of tendon allografts for reconstruction of the anterior cruciate ligament (ACL), Cell Tissue Bank 13 (3) (2012) 387–400.

[45] B. Lorber, F. Fischer, M. Bailly, H. Roy, D. Kern, Protein analysis by dynamic light scattering: methods and techniques for students, Biochem. Mol. Biol. Educ. 40 (6) (2012) 372–382.

[46] V.M. Borderie, P.-Y. Boëlle, O. Touzeau, C. Allouch, S. Boutboul, L. Laroche, Predicted long-term outcome of corneal transplantation, Ophthalmology 116 (12) (2009) 2354–2360.

[47] F. Luengo-Gimeno, D.T. Tan, J.S. Mehta, Evolution of deep anterior lamellar keratoplasty (DALK), Ocul. Surf. 9 (2) (2011) 98–110.

[48] S.V. Patel, J.W. McLaren, D.O. Hodge, W.M. Bourne, The effect of corneal light scatter on vision after penetrating keratoplasty, Am. J. Ophthalmol. 146 (6) (2008) 913–919.

[49] S.S. Shanbhag, H.N. Saeed, E.I. Paschalis, J. Chodosh, Boston keratoprosthesis type 1 for limbal stem cell deficiency after severe chemical corneal injury: a systematic review, Ocul. Surf. 16 (3) (2018) 272–281.

[50] D. Srikumaran, B. Munoz, A.J. Aldave, J.V. Aquavella, S.B. Hannush, R. Schultze, M. Belin, E.K. Akpek, Long-term outcomes of Boston type 1 keratoprosthesis implantation: a retrospective multicenter cohort, Ophthalmology 121 (11) (2014) 2159–2164.

[51] S.S. Shanbhag, H.N. Saeed, E.I. Paschalis, J. Chodosh, Boston keratoprosthesis type 1 for limbal stem cell deficiency after severe chemical corneal injury: a systematic review, Ocul. Surf. 16 (3) (2018) 272–281.

[52] S.K. Bakshi, J. Graney, E.I. Paschalis, S. Agarwal, S. Basu, G. Iyer, C. Liu, B. Srinivasan, J. Chodosh, Design and outcomes of a novel keratoprosthesis: addressing unmet needs in end-stage cicatricial corneal blindness, Cornea 39 (4) (2020).

[53] L. Wang, Z. Li, T. Wu, A. Liu, X. He, S. Zheng, T. Ye, L. Rong, Y. Huang, Modified Boston type-II keratoprosthesis implantation with autologous auricular cartilage reinforcement, Ocul. Surf. (2020).

[54] M.C. Robert, S.N. Arafat, J.B. Ciolino, Collagen cross-linking of the Boston keratoprosthesis donor carrier to prevent corneal melting in high-risk patients, Eye Contact Lens 40 (6) (2014) 376–381.

[55] F. Raiskup, E. Spoerl, Corneal crosslinking with riboflavin and ultraviolet A. I. Principles, Ocul. Surf. 11 (2) (2013) 65–74.

[56] E. Spoerl, G. Wollensak, T. Seiler, Increased resistance of crosslinked cornea against enzymatic digestion, Curr. Eye Res. 29 (1) (2004) 35–40.

[57] C.R. Rowland, K.A. Glass, A.R. Ettyreddy, C.C. Gloss, J.R.L. Matthews, N.P.T. Huynh, F. Guilak, Regulation of decellularized tissue remodeling via scaffold-mediated lentiviral delivery in anatomically-shaped osteochondral constructs, Biomaterials 177 (2018) 161–175.

[58] C.P. Sharma, Biointegration of Medical Implant Materials, Woodhead Publishing, 2019.

[59] S.S. Tuli, G.S. Schultz, D.M. Downer, Science and strategy for preventing and managing corneal ulceration, Ocul. Surf. 5 (1) (2007) 23–39.

[60] J.Y. Oh, J.M. Yu, J.H. Ko, Analysis of ethanol effects on corneal epithelium, Invest. Ophthalmol. Vis. Sci. 54 (6) (2013) 3852–3856.

[61] H.-Y. Liu, P.-T. Yeh, K.-T. Kuo, J.-Y. Huang, C.-P. Lin, Y.-C. Hou, Toxic keratopathy following the use of alcohol-containing antiseptics in nonocular surgery, JAMA Ophthalmol. 134 (4) (2016) 449–452.

[62] S.Y. Kim, W.J. Sah, Y.W. Lim, T.W. Hahn, Twenty percent alcohol toxicity on rabbit corneal epithelial cells: electron microscopic study, Cornea 21 (4) (2002) 388–392.

[63] H.S. Dua, R. Deshmukh, D.S.J. Ting, C. Wilde, M. Nubile, L. Mastropasqua, D.G. Said, Topical use of alcohol in ophthalmology - Diagnostic and therapeutic indications, Ocul. Surf. 21 (2021) 1–15.